5 Superconductivity: 2D Physics, Unknown Mechanisms, Current Puzzles

Warren E. Pickett

Department of Physics, University of California Davis

Davis CA 95616, U.S.A.

Contents

1   Overview: why this topic? what kinds of correlated states?

Superconductivity has been beguiling and bedeviling physicists for a century while numerous other quaint and curious collective phenomena have been discovered and analyzed, yet it maintains its mystery in spite of the enormous amount that has been learned and the vast competition for the physical scientist's attention and devotion. Levitation of a magnet over a superconductor, or vice versa, that can be turned on and off by temperature around the critical temperature T_c, and by anyone with a liter of liquid N_2, fascinates the viewing public (and often we practitioners as well). The "mysteries" of superconductivity – why do the high T_c members have such impressive behavior; can T_c be elevated closer to, or even above room temperature – combine with the unfilled promises of applications of room temperature superconductors to keep this area of study alive in the minds and the laboratories of a large number of scientists.

Though it may surprise the reader, there will be no description or analysis in this article of either the high temperature superconducting (HTS) cuprates, with T_c of 130+ K increasing to 160+ K under pressure, nor of the more recent Fe-based HTS superconductors (FeSCs) with T_c as high as 56 K. Neither will heavy fermion superconductivity be discussed. The emphasis in this overview will be on demonstrating that there are other classes of superconductors that are perplexing: their pairing mechanisms are not understood but seem different from the heavily studied classes, hence they are candidates to lead to new classes of high temperature superconductors. The focus here will be a much quieter area of superconducting materials and associated phenomena: strongly two dimensional (2D) band insulators where doping leads to superconductivity and, at least for several, the mechanism seems unrelated to magnetism. We will ask: what are the peculiar superconductors that beg for explanation; what are the characteristics that set them apart from other classes; what types of electron-electron (and electron-ion) correlations determine their behavior? An additional reason for this choice of emphasis is that, after more than 25 years of intense study of the cuprate HTSs and a huge amount of publications, a brief overview would serve little purpose. The intense study of the FeSCs is ongoing, involving numerous issues, and one should have similar reservations about attempting a brief overview.

The pairing mechanism in the cuprate and iron-based HTSs must be magnetism-related, due to the evident competition between magnetic order and superconductivity. Pinpointing of the mechanism, and why the cuprate and pnictide structures and characteristics are so special (HTS, with T_c above 50 K, occurs only in these two classes), remains one of the outstanding theoretical conundrums in materials physics. The Babel-istic situation was illuminated by Scalapino in his synopsis of the Materials and Mechanism of Superconductivity M^2S-HTSC conference (Dresden, 2006). He noted that, by his compilation, the "mechanisms" that had been discussed *at that conference alone* included: (a) Jahn-Teller bipolarons; (b) central role of inhomogeneity; (c) electron-phonon + U; (d) spin fluctuations; (e) charge fluctuations; (f) electric quadrupole fluctuations; (g) loop current fluctuations; (h) d density wave; (i) competition between competing phases; (j) Pomeranchuk instabilities; (k) d-to-d electronic modes; (l) RVB-Gutzwiller projected BCS. Learning more about these various terminologies will be left to the interested researcher, but it clear that there is a profusion of concepts and a paucity of consensus on the
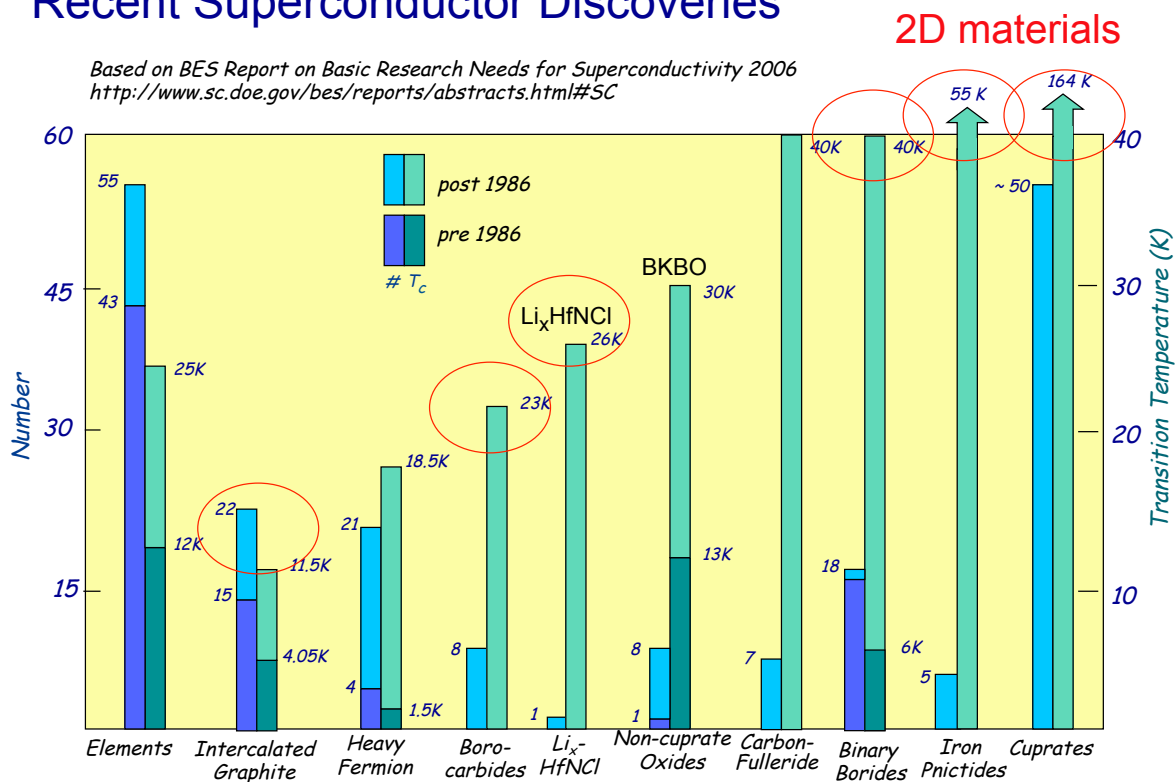
Fig. 1: *Plot of data relating to the main classes of high temperature superconductors. Note the legend (upper part of figure): for each class, # means the number of members, T_c gives the maximum critical temperature; bottom part of bar indicates pre-1986 (HTSC breakthrough), upper part of bar indicates post-1986. The main relevance for this paper is emphasized by the red ellipses, which identify the classes with substantial 2D character. The borocarbides have been included as 2D because of the strong layered aspect of their crystal structures; they are however 3D metals. Most of the classes of HTSs are quasi-2D, without any clear connections between most of the classes. Courtesy of George Crabtree; based on data available in 2006.*

microscopic mechanism of pairing of cuprate HTS.

2   Very basic theoretical background

Practically all theories of superconductivity draw on the basic, Nobel Prize winning theory of Bardeen, Cooper, and Schrieffer (BCS theory [1]). They presumed that there is some effective attraction between electrons (for them, it was due to exchange of virtual phonons, though such details were peripheral) that provided the opportunity for Cooper pairs [2] to form and to spon-

taneously condense into a collective non-Fermi liquid state – the superconducting condensate – in which these pairs become correlated into a coherent many-body phase. Cooper had just demonstrated [2] that the Fermi liquid ground state is unstable toward the formation of a single such pair, even if the pairing strength is arbitrarily small. A reading of the BCS paper [1] is a must for any student of physics who wishes to acquire a basic understanding of the super-conducting state, the spectra, and the low energy, low temperature (T) thermodynamics. The diligent student should even work her way through at least the first ten pages or so of the al-gebra – it tremendously helps understanding to know something about how the processes are described algebraically.

2.1 Weak coupling

In BCS theory, there is an electronic density of states N(0) at the Fermi level, presumed to vary slowly on the scale of the energy of the virtual boson that transmits the interaction (viz. phonon, in conventional superconductors). The attractive effective interaction $-V$ ($V > 0$) is presumed to be constant up to a cutoff $\hbar\omega_c$ of the order of a phonon energy. The approach used by BCS was to guess the form of a correlated ground state wavefunction depending simply on few parameters, and obtain the parameters via a mean-field minimization of the energy, first at T=0 and then at finite temperature. Conventional SCs, by the way, are exceedingly good examples of "mean field transition" systems, the critical region around T_c being exponentially small and unobservable. In the weak coupling limit, and only in that limit, T_c is exponentially related to coupling strength λ:

$$k_B T_c = 1.14\hbar\omega_c e^{-\frac{1}{\lambda}}; \quad \lambda = N(0)V. \tag{1}$$

At moderate $\lambda \sim 0.5$-0.75, say, the equation must be solved numerically for T_c, and $T_c(\lambda)$ is quasilinear rather than exponential. The strong coupling regime must be treated separately and is discussed below.

The superconducting gap is constant over the nondescript Fermi surface (FS) in the broadest form of BCS theory. The more general expression for the momentum dependence of Δ_k over a general FS is given by [3]

$$\Delta_k = -\sum_{k'} V_{k,k'} \frac{\Delta_{k'}}{2\sqrt{\varepsilon_{k'}^2 + \Delta_{k'}^2}} tanh \frac{\sqrt{\varepsilon_{k'}^2 + \Delta_{k'}^2}}{2k_B T} \to -\sum_{k'}^{FS} V_{k,k'} \frac{\Delta_{k'}}{2\sqrt{\varepsilon_{k'}^2 + \Delta_{k'}^2}}, \tag{2}$$

where the last expression is the T→0 expression. More generally, band indices are also required. The $tanh$ term arises from Fermi-Dirac thermal distribution factors, ε_k is the non-interacting band energy, and $V_{k',k}$ is the matrix element for scattering of pairs between k and k' on the Fermi surface. The critical temperature T_c is determined from linearized gap equation in the limit of $\Delta_k \to 0$:

$$\Delta_k = -\sum_{k'}^{FS} V_{k,k'} \frac{\Delta_{k'}}{2\varepsilon_{k'}} tanh \frac{\varepsilon_{k'}}{2k_B T} \tag{3}$$

T_c is the highest temperature for which there is a nonvanishing solution for Δ_k.

Although these gap equations (finite T and the linearized version giving T_c) are in the weak coupling limit (and subject to other simplifications made in BCS theory), they are very commonly applied, or at least cited, in situations where they have not been justified. This reflects the confidence that theorists have that some "essence" of pairing superconductivity is contained in these equations. The linearized equation Eq. 3 is especially prevalent in modern discussions. With the discovery of the HTS cuprates, there quickly arose a great deal of interest in Fermi surface nesting, in hot spots on the Fermi surface (van Hove singularities extending toward infinity), and in pairing interactions in which there is *strong anisotropy*. This anisotropy usually does not become important for electron-phonon pairing, but if one assumes that magnons can induce pairing analogously to phonons – the virtual boson that is exchanged is a magnon rather than a phonon – then anisotropy becomes paramount. In the cuprates, it is presumed that (1) the strong Coulomb repulsion U on Cu keeps potentially pairing electrons off the same Cu site, and (2) the interaction is dominated by strong short-range AFM fluctuations.

The influence of the linearized gap equation Eq. 2 on contemporary superconductivity theory can hardly be overemphasized. In BCS theory the (maximally isotropic) coupling must be *attractive* to obtain solutions of the gap equation. When the interaction is anisotropic and even repulsive on average, gap solutions (*i.e.* superconducting states) for non-zero Δ_k can still be obtained. The change of sign with angle of the pairing interaction can be compensated by a change in sign of Δ_k with angle. The quantity under the integral in Eq. 2 and Eq. 3 is then predominantly of one sign, as is the case of an attractive isotropic coupling and isotropic gap. The interested student or postdoc will benefit in understanding by studying the above gap equations by expanding the various functions in spherical (3D) or circular (2D) harmonics, and making reasonable assumptions about the behavior with the magnitude of $|k - k_F|$ (constant up to a cutoff, say). Looking at the linearized case T→T_c and contributions from the Fermi surface $\varepsilon_k \rightarrow 0$ are most useful. Expressions for general FSs (number and shape) can be written down using the Fermi surface harmonics of Allen, [4] although all but the simplest situations will require numerical solution.

These anisotropic gap solutions are a realization of the "theorem" of Kohn and Luttinger, [5] which pointed out that such anisotropic solutions would exist for anisotropic coupling, although at the time they were expected to have implausibly small values of T_c. Such *exotic pairing*, or *exotic order parameter*, has become over the past two decades commonplace in theories and have found strong confirmation in cuprates and some heavy fermion SCs. Several experiments demonstrate (or strongly imply) that the hole-doped cuprates have a d-wave order parameter (gap function Δ_k), with angular dependence like $sgn(x^2 - y^2)$; thus it is referred to as a $d_{x^2-y^2}$ (angular momentum of the pair $\ell = 2$) symmetry order parameter for the superconducting state. In heavy fermion superconductors, $\ell = 3$ pairing seems likely [6] in UPt$_3$, which has hexagonal symmetry that conspires against d-wave symmetry. In considering new superconductors, one of the most valued characteristics is determining if pairing is "conventional" (isotropic $\ell = 0$) or "exotic" (anisotropic $\ell > 0$), because this character is likely to reflect conventional electron-phonon or unconventional pairing, respectively. In the latter case the gap (usually) has nodes on the Fermi surface, hence there is no true gap in the superconductor's excitation spectrum. This

aspect impacts thermodynamics strongly, and the temperature dependence of thermodynamic quantities as T→0 is the most common evidence quoted for the (an)isotropy of pairing. If there is a gap, the heat capacity goes exponentially to zero as T→0, if not it approaches zero as a power law in temperature.

2.2 Strong coupling

Strong coupling indicates the regime $\lambda \geq 1$ where perturbation theory in the electron-phonon coupling strength no longer holds, and many aspects of the physics are different. For the phonon mechanism, the generalization of Eliashberg [7] of BCS theory to strongly coupled electron-phonon models was extended into an extremely detailed and strongly nuanced, material-specific formalism by Scalapino, Schrieffer, and Wilkins. [8] It is this generalization that is now commonly referred to as strong coupling *Eliashberg theory* (as opposed to weak coupling BCS theory). Together with the introduction, at the same time, of density functional theory (DFT) by Hohenberg, Kohn, and Sham [9,10] and its subsequent very extensive development, DFT-based Eliashberg theory has been shown repeatedly to describe phonon-paired superconductors quite reliably. The primary restriction for the applicability of Eliashberg theory is that the effective Coulomb repulsion between electrons is retarded in time and is weak, thus it can be characterized by a repulsive effective interaction strength $\mu^* = 0.1 - 0.2$. When the impact of the Coulomb interaction is great, which usually manifests itself in magnetic behavior, no justifiable theory of superconductivity exists.

Within DFT-Eliashberg theory the electron-phonon interaction (EPI) strength is given for an elemental metal by

$$\lambda = \frac{N(0)I^2}{M\langle\omega^2\rangle} \equiv \frac{K_e}{K_\ell}; \quad I^2 = \langle\langle V_{k,k'}^2\rangle\rangle. \tag{4}$$

Here $V_{k,k'}$ is matrix element for scattering from the FS (k) to the FS (k') by an atomic displacement, M is the ionic mass, and the phonon frequency average is weighted appropriately by matrix elements. This expression is precisely true for elemental SCs (note that only one mass enters) but survives as a guideline for compounds where the character of coupling can be much richer. This form emphasizes that λ represents the ratio of an "electronic stiffness" K_e and the (textbook) lattice stiffness K_ℓ, *i.e.* determined by the interatomic force constants. For a harmonic lattice the product $M\langle\omega^2\rangle$ is independent of mass, so the mass dependence of T$_c$ comes solely from the prefactor $\omega_c \propto 1/\sqrt{M}$. This mass dependence reflects a crucial factor in EPI-based pairing that has been recognized and exploited since the prediction that metallic hydrogen should be a room temperature superconductor: other factors *i.e.* the electronic structure, being the same, materials with lighter ions should have higher T$_c$ simply because the fundamental energy scale ω_c is higher.

Strong coupling Eliashberg theory is much richer than BCS theory. Allen and Dynes [11] analyzed materials trends and the Eliashberg integral equation for T$_c$ and demonstrated, among other results, that at large coupling T$_c \propto \sqrt{\lambda}$ and thus is unbounded, providing strong encouragement for the likelihood of (much) higher T$_c$ SCs. Since this article will not deal with issues

of strong coupling, this and other aspects of Eliashberg theory are not needed for the discussion and will not be presented here.

3   Doped 2D ionic insulators: general aspects

3.1   A broad view of the theoretical challenge

Conventional pairing, that is, electron-phonon, is fully attractive: every phonon contributes to an *attractive* interaction between electrons on the Fermi surface. This attraction also operates in unconventionally paired superconductors (such as the HTS cuprates) but seems to be inef-fective. It may even be detrimental to the eventual superconducting state if the gap symmetry is exotic. The always attractive electron-phonon interaction strongly favors a fully symmetric gap, although highly anisotropic pairing and complex FSs might provide more interesting order parameter symmetry. The screened Coulomb interaction between electrons is *almost always repulsive*, but the average repulsion may become irrelevant if pairing is anisotropic, according to current understanding, and the Kohn-Luttinger result mentioned earlier.

The purpose of this article is to provide an overview of a few classes of materials – 2D doped ionic insulators – wherein the Coulomb interaction between electrons, normally repulsive, may acquire new traits beyond what have been studied thoroughly so far. Two dimensionality may play a special role, [12] through the phase space that it carries and the manner in which interac-tions are shaped. A relatively low density of doped-in carriers may introduce novel dynamical effects. And when these two aspects are present in the background of highly charged, vibrating ions, the underlying behavior may include unusual emergent aspects (to use a term much in fashion these days).

3.2   Density of states N(E); generalized susceptibility $\chi(q)$

Near a band edge with normal quadratic dispersion in 2D, the density of states N(E) is a step function. Thus small doping leads already to a large, metallic value of N(0) unlike in 3D semimetals where N(0) increases monotonically with the carrier concentration and may be arbi-trarily small at low doping. It is for this reason that B-doped diamond becomes superconducting but with only a modest value of T_c (up to 11 K has been reported [13]). In other respects this system is in the MgB_2 class (more specifically, the hole-doped LiBC) class, where electron-phonon matrix elements are large and the relevant phonon frequency is very large.

Due to the 2D character, the FSs are closed curves versus the closed surfaces that occur in 3D. Near a band edge these will be circles or nearly so, making their algebraic description and even that of the complex generalized susceptibility $\chi(Q,\omega)$ possible. [14] Thus the underly-ing mean-field, static lattice electronic structure and linear response is straightforward, even simple, to model. $\chi^{2D}(Q,\omega)$ is available analytically for a single circular FS, and for a few symmetry-related FSs, which comprise a multi-valley system, this χ^{2D} for a single band will be supplemented by a sum of inter-FS terms $\chi^{2D}(|Q - Q_s|,\omega)$, the same form but for initial

and final FSs separated by the spanning wavevector(s) Q_s. (If band extrema do not occur at high symmetry points, the FSs may be ellipsoidal instead of circular and the form of $\chi(Q, \omega)$ becomes anisotropic and correspondingly more involved.

3.3   Electronic screening by a sparse electron gas

Due to electronics applications of 2D electron gases (2DEGs), the dynamical response of 2DEGs has been studied extensively. Within the random phase approximation (RPA), the plasmon dispersion is given implicitly by $\epsilon(Q, \omega_p) = 1 - v(Q)\chi(Q, \omega_p) = 0$ where $v(Q)$ is the Coulomb repulsion; that is, a "response" can occur in the absence of any perturbing potential when the screening ϵ^{-1} diverges. Whereas the usual long wavelength plasmon in 3D behaves as $\omega_p^2(Q) = \omega_p^2(0) + BQ^2 + ...$, in 2D the much stronger dispersion $\omega_p = A\sqrt{Q} + ...$ holds. The plasmon vanishes at Q=0, leading to strong dynamical behavior (screening, perhaps over-screening or other unconventional behavior) in at least a small region around Q=0. The idea that 2DEGs might be fertile ground for superconductivity has been around for some time. [12] Ionic insulators have high frequency TO and LO modes also around Q=0 that will cross and interact with the plasmon, leading to coupled modes that are candidates for unconventional dynamical behavior and possible pairing of electrons. Layered crystals do not present strict 2DEGs however; they are instead (naturally occurring, or nowadays sometimes grown atomic layer by layer) multilayers. In the multilayer case the Coulomb interaction couples the response of neighboring layers (even in the absence of electron hopping between layers) and the $Q \to 0$ plasmon remains finite [15] but may still be very soft and strongly coupled to ionic dynamics.

3.4   Dynamics of the coupled ion-electron system

Allen, Cohen, and Penn [16] (ACP) have emphasized that the total interaction between two electrons in a crystal involves the combined dynamic polarizability (*i.e.* the total dielectric function) of the electronic system and the lattice, and they have provided a firm background for the study of such systems. When the conduction electron density is low, the competition between weakly, dynamically screened repulsive (electron-electron, cation-cation, anion-anion, electron-anion) and attractive (electron-cation, anion-cation) interactions may produce new "regions" of effective attraction. They derived within a general formalism that can be approached in a material-specific, first principles way (such as by using a DFT starting point) that, even taking into account interactions between electrons, between ions, and between ions and electrons, that the polarizability of the system is the sum of two terms: that of the vibrating ions, and that resulting between electrons interacting through the dynamically screened Coulomb interaction. Bill and collaborators [17, 18] have constructed the most detailed model of 2D superconductivity arising from coupled phonon-plasmon modes, giving particular attention to special aspects of plasmonics in two dimensions. Related themes appear occasionally elsewhere in the literature, for example that of Askerzade and Tanatar [19] and of Falter and coworkers. [20, 21] Other unconventional interaction channels may arise is such systems. Ashcroft has emphasized polarization waves due to flexible semicore electrons [22] as possibly contributing to pairing.

In 2D lattices where there is a natural axis (the c axis), polarization modes ("ferroelectric fluctuations") may have more impact than in 3D lattices.

4   Electron-phonon coupling in 2D HTS metal MgB$_2$ class

One focus of this article is two dimensionality and its relation to superconductivity and T$_c$, so it is important to review (albeit briefly) the spectacular surprise presented by MgB$_2$ in 2001 by Akimitsu's group. [23] The account of the quest for other MgB$_2$-like materials, following in Sec. 3.2, is both intriguing and sobering.

4.1   The surprise of MgB$_2$

This standard sp HTS metal, with T$_c$=40 K when the light isotope of B is used, is described well by Eliashberg theory (in its multiband extension), as implemented in DFT-based electron-phonon calculations. [24–28] It provided many lessons by violating nearly all of the conventional wisdom of the time: (a) it is an sp, not d metal; (b) it is strongly 2D rather than 3D; (c) it becomes a HTS superconductor due to *extremely* strong coupling to *extremely* few (3%) of the phonons, rather than having the strength spread rather uniformly over the phonon spectrum. It is best regarded not a standard metal, but as a self-doped semimetal; the crucial σ-bonding band is nearly filled. The basic aspects of the electronic structure and coupling – that high frequency B-B stretch modes are extremely strongly coupled to the strongly bonding B-B states at the Fermi surface – can be well understood in terms of simple formal expressions, which provides an explicit recipe [29, 14] for the type of extension from MgB$_2$ that could provide much higher T$_c$ within this class of metal. The concept is provided briefly in Fig. 2 and its caption. Simply put, change the Fermi surfaces to make use of coupling to more phonon modes and provide a larger electronic density of states, while retaining the structure that gives very strong bonding (large electron-phonon matrix elements).

4.2   Superconductor design: attempts within the MgB$_2$ class

The simplicity of the crucial features of MgB$_2$ has encouraged discovery or design of additional members of this class of superconductor, as described briefly in this subsection.

4.2.1   Hole-doped LiBC.

The first such proposed extension fits in with the focus of this article in many respects, except for the fact that electron-phonon coupling is not really a focus. LiBC is isostructural and "isovalent" with MgB$_2$ (Li having one less electron than Mg, C having one more electron than B), but it is insulating due to the inequivalence of B and C on the honeycomb sublattice. Hole-doping in this covalent/ionic insulator by partial removal of Li, while retaining the crystal structure and obtaining a black (likely conducting) sample, was reported by Wörle *et al.* [30] in 1995. Calculations of the electron-phonon coupling strength by Rosner *et al.* predicted that such
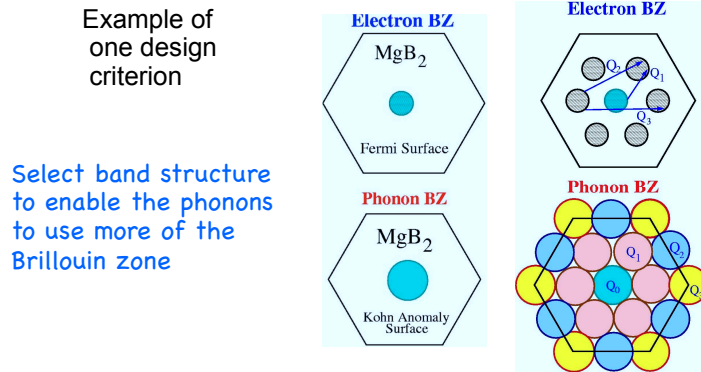
Fig. 2: *A proposal for rational design of higher T_c materials. Rational design is possible because the electron-phonon interaction and resulting superconductivity is extremely well understood (in weakly correlated Fermi liquid metals). MgB_2 makes use of extremely strong coupling $\lambda_{q\nu}$=20-25 to only 2-3% of the phonon modes: the two bond stretch modes polarized in the plane (hence 2 of 9 branches) in only 8% of the zone (where $q < 2k_F$). Adding Fermi surfaces in other parts of the zone provides coupling from branches at other values of q: Q_1, Q_2, Q_3 connecting the various sheets of Fermi surface. A nearly ideal scenario is pictured on the two zone figures on the right. See Refs. [29, 14] for further description.*

doping would lead to T_c of 75 K or higher. [31, 32] $Li_{1-x}BC$ is a MgB_2 look-alike system, with the increase in T_c over that of MgB_2 being due to the stronger B-C bonding compared to B-B bonding in MgB_2, giving both larger matrix elements and a higher phonon energy scale. Work on this system, with the most extensive being done by the Rosseinsky group, [33] indicates unfortunately that the doped system is prone to (structural and phase separation) instabilities that prevent realization of the desired phase. The report of Wörle *et al.* has never been confirmed. Lazicki and collaborators [34] pursued the possibility that pressure might close the gap and induce metallization and thereby superconductivity. The structure remained stable to 60 GPa, and density functional calculations predicted that metallization in this structure would not occur until at least 345 GPa. This system illustrates how higher T_c is in practice often limited by instabilities that can appear in assorted flavors, while the underlying theory provides no upper limit [11] on the possible value of T_c.

4.2.2 Transforming graphite into pseudo-MgB_2

Simultaneously with the study of $Li_{1-x}BC$, our group considered a different means to obtain an MgB_2-like material. MgB_2 is, after all, graphite with an extra three dimensional band in the

background. The difference is that MgB_2 has a different potential between the honeycomb layer and the interstitial, or Mg, layer. The σ-bonding band is present in graphite, but its upper edge is 2 eV below the Fermi level, which is determined by the positioning of the π-bonding band at the symmetry point K in the Brillouin zone, which has in the meantime asserted its infamy in the plethora of graphene research of the past decade. Our idea was simple – in hindsight, it was simplistic. What seemed to be necessary was to lower the Fermi level by 2 eV in graphene. This could be done by intercalating it with a highly electronegative ion. The most electronegative one, and also a small one, is fluorine. Joonhee An [35] carried out the calculation of FC_2 in the MgB_2 structure. Fluorine did become a negative ion of course, but another change that we had not anticipated was a shift in Madelung potential. This shift counteracted to a great degree the charge transfer, and left the Fermi level well away from the σ-bonding bands. Thus this approach to HTS design did not work.

4.2.3 Hole-doped MgB_2C_2.

The (unsuccessful) example of LiBC has encouraged further exploration into this direction of finding MgB_2-like materials. The borocarbide compound MgB_2C_2 is isovalent to, and structurally similar to, the (super)conductor MgB_2 and to insulating LiBC. The structure [36] is pictured in Fig. 3 (see the caption for more description). Due to the placement of Mg ions, the honeycomb B-C layers are dimpled somewhat. Density functional based electronic structure calculations and electron-phonon coupling strength calculations [37–41] show that MgB_2C_2 (i) is insulating like LiBC due to the modulation of the honeycomb B-C layers, (ii) exhibits a rather high B-C σ-band density of states close to the Fermi level when slightly hole doped, and (iii) shows a strong deformation potential with respect to the B-C bond stretching modes, as demonstrated in Fig. 3. If large enough hole doping of the system can be achieved, such as by replacement of Mg by Li, it should be superconducting at temperatures comparable to MgB_2. Mori and Takayama-Muromachi reported attempts to hole dope this compound both on the Mg site and within the B-C network, but found no indication that the dopants actually entered the crystal structure. [42] Yan and collaborators [43] have recently provided an extensive density functional study of the structural and thermodynamic properties of insulating MgB_2C_2.

4.2.4 Hole-doped BeB_2C_2.

Forty years after the compound was first synthesized, its structure was finally solved by Hoffman *et al.* [44] While possessing the same honeycomb B-C layers as LiBC and MgB_2C_2, it has a specific, non-intuitive stacking due the the position of the interlayer Be, which likes to coordinate on one side with a single C atom. Before the structure was known, Moudden calculated the electronic structure and electron-phonon coupling strength for a different structure also based on the B-C honeycomb rings. [45] Although the bands at the bottom of the gap, which are the active states when hole-doped, are considerably more intricate than MgB_2C_2, Moudden obtained a larger coupling strength and T_c than for MgB_2, for the same reasons as for hole-doped LiBC and MgB_2C_2. In our unpublished work [46] using the experimental structure, we find the
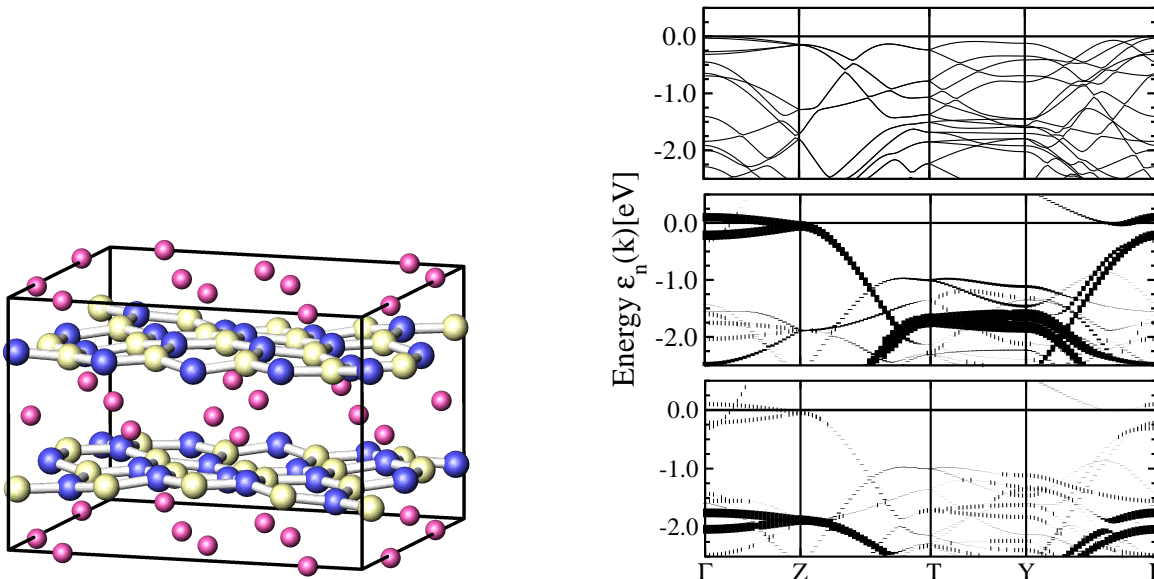
Fig. 3: *Left panel: the orthorhombic crystal structure of MgB_2C_2 in perspective view. Mg, B and C are represented by pink (small spheres) blue, and light yellow (larger) spheres, respectively. The buckling of the visualized covalent B-C bond causing the deviation from the ideal hexagonal plane is visible. Right panel: Band structure for the undistorted (upper subpanel) and B-C σ 'fat bands' for a frozen-in bond stretching phonon (middle and lower subpanels) with a bond elongation around the rms value. The large energy difference between the $2p_x$ orbitals (middle panel) and the $2p_y$ orbitals (lower panel) indicates the very strong deformation potential for this mode. From H. Rosner, A. Kitaigorodsky, and W. E. Pickett, unpublished.*

relevant bands are simpler than those obtained by Moudden, and in fact much more MgB_2-like. Not surprisingly, we also obtain very strong coupling to the B-C stretch modes and a probable T_c higher than in MgB_2.

4.2.5   Comments on this class of doped insulators.

MgB_2 has spawned the study of these hole-doped ABC and AeB_2C_2 insulators (A = alkali; Ae = alkaline earth), which has led to theoretical prediction of high temperature superconductivity. This activity has been disappointingly unproductive so far, which in the cases attempted experimentally has been stymied by inability to introduce the dopant (or the vacancy) in a random alloy fashion as presumed by the theory – chemistry gets in the way. A further member, CaB_2C_2, also exists. [47] It also sports a 2D B-C network, but one comprised of B-C octagons and B-C diamonds rather than the honeycomb network of the others. This system certainly seems worthy of study and attempts at doping.

This progression from the 2D B-B net of MgB_2 to the B-C nets of the Ae compounds can be taken a step further: the network components can be changed from B-C to Be-N, substantially increasing their distance in the periodic table and thereby reducing the degree of covalency while retaining the overall isovalent nature. The compounds are indeed insulating, and Ae = Ca, Sr, Ba have the same structure as CaB_2C_2. The Ae = Mg compound has a distinctive structure

built on a strongly puckered Be-N bilayer with Mg ions distributed between the layers. [48]

5   Doped 2D ionic insulators: examples

5.1   Transition metal nitridochlorides HfNCl and ZrNCl

The class $\mathcal{T}$NCl, where $\mathcal{T}$ is a group IVB transition metal Hf, Zn, and Ti, and having a few Br (instead of Cl) members, is the prime example of the type of superconductor that will receive emphasis in the remainder of this article. These three isovalent compounds display T_c up to 25.5 K, 15.5 K, and 17.5 K respectively when electron doped. [49–54] None have been hole doped, and the active states in that case would be very different, being N $2p$ states. Undoped, they are highly ionic $\mathcal{T}^{4+}N^{3-}Cl^{+}$ moderate gap ($\sim$2-3 eV) insulators with strongly layered structures. The $\mathcal{T}$ = Hf and Zr members, which are extremely similar in electronic structure, have a somewhat dimpled BN-like alternating honeycomb -Hf-N-Hf-N- bilayer with Hf-N bonds coupling the bilayers. Cl caps the honeycomb holes above and below, resulting in neutral layers that are van der Walls bonded.

The covalence between the d states and the N $2p$ states in these ionic compounds is evident in their Born effective charges (BECs). The BECs are highly anisotropic, often differing by a factor of two between in-plane and out-of-plane, and in some cases the values are well above (in magnitude) their formal charges. [55] The trend in magnitudes increases from $5d$ to $3d$. It is these values, and the internal electric fields that result, that a small amount of carriers will experience.

Alkali ions, without or with larger organic molecules, can be intercalated between the layers to induce conductivity and superconductivity, and recently it has been shown that (trivalent) rare earths can also be used for the doping, with T_c remaining the same. Once somewhat beyond the insulator-superconductor transition, [56] T_c is almost independent of the carrier density (the doping level). The layering and bonding of the TiNCl compound is very similar, although the crystal symmetry is orthorhombic rather than hexagonal/rhombohedral as are the others. We return to TiNCl in the next subsection. Schurz *et al.* [57] have provided a recent experimental overview of these materials, primarily on synthesis and structure.

It was shown by Weht and coauthors [58] that the doped electrons are accommodated at the bottom of the $\mathcal{T}$ d band, which has substantial in-plane dispersion (the effective mass is of the order of unity) as shown in Fig. 4; see the caption for more explanation of the electronic structure. Thus due both to the broad d band and the small carrier concentration (far from half filling) the type of strong correlation effects that are ubiquitous in transition metal oxides appear not to be dominant in this transition metal nitride, and there is no experimental evidence of correlation effects such as magnetic moments and magnetic ordering, or orbital or charge ordering, etc. It was also found that the electronic structure of isostructural HfNCl and ZrNCl are extremely similar, yet their consistently observed transition temperatures differ by a factor of two: 25 K versus 12-13 K for ZrNCl over most of the doping range. The difference in T_c is the wrong sign to be a BCS isotope effect. The difference in T_c must then be related to other
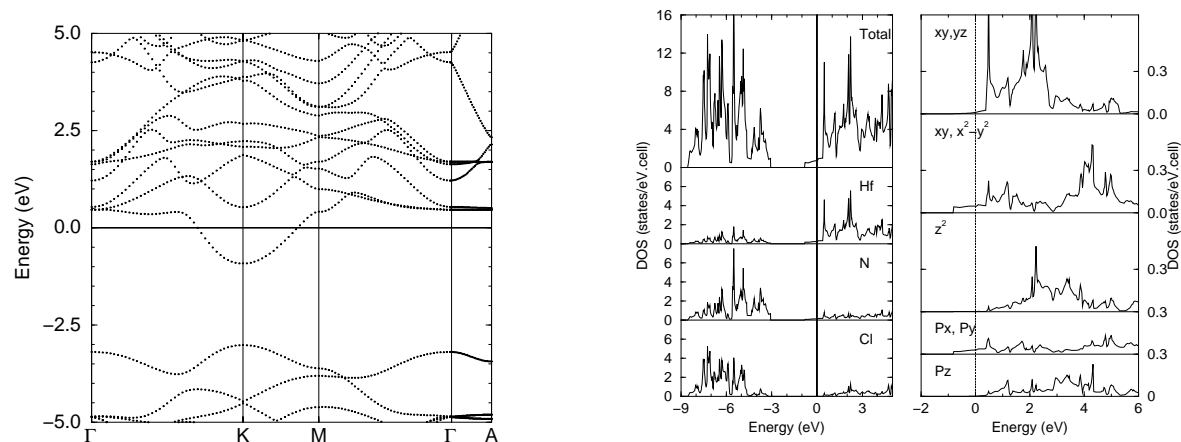
Fig. 4: *Left panel: Band structure of $Na_{0.25}HfNCl$ along the hexagonal symmetry lines, calculated in the virtual crystal approximation. The five bands above the gap are heavily Hf $5d$ in character, while the bands below are filled N^{3-} $2p$ bands. The Cl $3p$ bands lie somewhat deeper. The flatness along Γ-A indicates the very strong 2D character of the bands of interest. Right panels: The total, atom projected, and $5d$ and $2p$ projected densities of states. Note that the Fermi level lies in a region of rather low DOS of $d_{xy}, d_{x^2-y^2}$ character. The other three $5d$ bands lie $\sim$1 eV higher due to ligand field splitting. From Weht et al. [58]*

features: to differences in force constants or electronic response (*viz.* Born effective charges, or higher frequency response), though the similar band structures suggest they should not differ much, or to the factor of two difference in $\mathcal{T}$ mass (178 amu versus 91 amu) that affects lattice polarization.

Heid and Bohnen [59] carried out density functional linear response calculations of the el-ph coupling strength and character in A_xZrNCl in the same manner as is commonly done for Fermi liquid metals, and found the electron-phonon coupling $\lambda \approx 0.5$ is much too small to account for the observed value of T_c. Akashi *et al.* [60] have provided an application of "DFT for superconductors" to these nitridochlorides, and also conclude that something besides the usual Eliashberg theory is required to understand their superconductivity. This theoretical approach presupposes that (1) carriers are present in a weakly correlated Fermi liquid, and (2) doping can be treated in the virtual crystal approximation (VCA). VCA corresponds to adding charge without much concern how it got there, but treating it self-consistently, which can be important. [61] It is clear however that the materials are more complex than that. The most obvious evidence is from the observation that in Li_xZrNCl, metallic conduction does not occur until a critical concentration x_{cr}=0.06 is reached. [56] It is noteworthy that $x_{cr} = 0.15$ is different for the doped HfNCl compound, [62] however it should be kept in mind that the doping was done in a different manner. The VCA band structure remains, by supposition, that of a conventional Fermi liquid, however, to arbitrarily small doping levels. The interactions that keep the carriers localized at low doping are surely essential to address theoretically in this class of materials. For this, the Born effective charges [55] and perhaps nonlinear effects should be important. In addition, $T_c(x)$ in the Zr compound is maximum at x_{crit}, [56] about 25% higher than the value of $\sim$12 K over most of the measured range of x.

5.2   The TiNCl sister compound

α-TiNCl is an orthorhombic ($Pmmn$, #59) member of this class with the FeOCl prototype structure, with similarities and differences when comparing with the nitride halides in the previous subsection. It is a strongly layered compound including a double layer of Ti-N nets analogous to those of HfNCl and ZrNCl. Each net however has the topology of a single NaCl (001) layer rather than a honeycomb type, but the layers are displaced so Ti is coordinated with four N ions (two in the same layer, two in the other) and with two Cl layers above (or below). The layers are strongly buckled. The Ti-N bilayer is decoupled electronically from the bilayers above and below giving it 2D character, but the coordination and bonding are quite distinct from that of ZrNCl and HfNCl. More description, and references, are provided by Yin *et al.* [63]

The band gap of TiNCl is much smaller (0.5 eV) than that of its cousins, and also differs in having the gap occur at Γ rather than at the zone corner. Thus when electron-doped, there is a *single cylindrical Fermi surface* surrounding Γ-Z rather than two at the K and K' points. The character is again in-plane ($3d_{xy}$) and the band is $\sim$2 eV wide. The DOS near E$_F$, N(0), is similar to those of ZrNCl and HfNCl. And, of course, there is the fact that T$_c$ lies in the same, impressively high, range (17 K).

Yin *et al.* [63] assembled a tight binding model Hamiltonian based on Wannier functions and a Hubbard on-site repulsive interaction, and proceeded to calculate the charge and spin susceptibilities $\chi_{ijkl}^{c,s}(\vec{q})$, where the subscripts label the Wannier functions and lead to manifold functions. They presented a few elements that are expected to have the most weight in the full susceptibility, and noted that the approximate square symmetry of the Ti-N bilayer (at least when viewed from above) is strongly broken by some elements of this susceptibility matrix. The calculated Born effective charges are also strongly anisotropic in-plane as well as out-of-plane. The q-dependence of $\chi_{ijkl}^{c,s}(\vec{q})$ will be useful when measurements of the charge and spin fluctuation spectrum are available. They will also be useful if electronic, rather than phononic, mechanisms of pairing are considered.

5.3   Overview of these transition metal nitridohalides

It will be instructive to make a list of salient aspects of this class of superconductors, which is part of the broader class of *transition metal pnictide halides* that has been labeled "under explored." [64] Such a list should contain several clues about the origin of their remarkable superconductivity and more generally about the importance of two dimensionality and doping into ionic insulators.

- The occurrence of superconductivity and the value of T$_c$ is weakly dependent on the type and amount of doping, indicating a robust feature that is insensitive to details such as stacking of successive ($\mathcal{T}$NCl)$_2$ layers or manner of doping. ZrNCl can even be doped with Cl$^-$ vacancies to superconduct at 12-14 K, [65] which is the same range of T$_c$ that arises from alkali atom intercalation.

- In-plane symmetry seems to be of little consequence. The Hf and Zr members have

hexagonal, isotropic symmetry in the $a - b$ plane, while the Ti member has strongly anisotropic Born effective charges and susceptibilities with rectangular, anisotropic symmetry.

- A relatively large critical concentration of carriers (x_{cr}=0.06 for Li$_x$ZrNCl) is required for the insulator-to metal/superconductor transition. At lower concentrations, the doped in electrons are "solvated" into the transition metal bands, presumably as immobile polarons. This concentration corresponds to two carriers in each 4×4 supercell of ZrN bilayers, a low but not truly sparse carrier density. The 2D density parameter is $r_s \sim 20/\sqrt{\epsilon}$, where ϵ is the background dielectric constant of the insulator.

- T$_c$ is maximum in Li$_{1-x}$NCl at the metal-insulator transition at x_{cr}=0.06, as discussed above. This is surely an important clue, given that T$_c$ is so insensitive to other factors (interlayer spacing, type of dopant, doping level). This fact also prompts the question: can x_{cr} be decreased in some (otherwise innocuous) manner, and if so will T$_c$ continue to rise as the doping level decreases?

- The N isotope effect has been reported [66] to be 0.07±0.04, reflecting little dependence on N mass. This is quite small and uncertain, but possibly nonzero. Note that the actual shift ΔT$_c$ was 0.06±0.03K, which is nearing the limit of clear detectability. In any case, the N isotope effect is at least extremely small.

- The factor-of-two difference in T$_c$ between the Hf and Zr compounds invites study; so far there are not even any reasonable speculations on the origin of this difference. The electronic structures are nearly indistinguishable. Interpreted as an isotope effect, (1) the value is very large but also of the wrong sign, and (2) the difference in T$_c$ is as large as one of the T$_c$s, so an isotope exponent that assumes ΔT$_c$/T$_c$ is small is an inappropriate representation. Since the electron-phonon λ (evaluated in the usual manner) is seemingly small, there is little reason to expect this to be a standard isotope shift anyway.

- TiNCl has an analogous band structure and a metal-nitride bilayer also, and has T$_c$ midway between its two cousins. Yet the lattice symmetry and the Fermi surfaces are different. Supposing the pairing mechanism is the same, these similarities and differences provide clues and potential insight for the microscopic behavior impacting superconductivity.

- The Born effective charges [55] provide the electrodynamic effects of the vibrating charged ions in the weakly screened limit. If some correlation can be found between these charges and superconducting characteristics, it could provide important clues to the pairing mechanism.

5.4   Related classes of materials

One can guess that there must be a substantial number of 2D ionic band insulators that make reasonable candidates for superconductors when doped. We provide some brief comments here. $BaHfN_2$ seems to be a minor variant of the TNCl class. It structure is analogous, having transition metal nitride (Hf-N) layers bounded by the more ionic layers, which in this case contain BaN. [55] The electronic structure is analogous: N $2p$ states are filled, and the conduction band states that are available for electronic carriers above a (calculated) gap of 0.7 eV are Hf $5d$ states, hybridized with N $2p$ states. This compound differs from the TNCl class in a way that may be important for synthesis: it has only a single reactive anion (N). Many 2D materials are grown layer by layer by sputtering, plasma laser deposition, or molecular beam epitaxy. Much experience has been gained in dealing with multiple cations in the chamber, but usually a single anion is used (and that is almost always oxygen).

The sister compounds $SrZrN_2$ and $SrHfN_2$ have also been synthesized. [67] The growth in nitride synthesis has led to an expanding number of transition metal nitrides, many of which have strongly 2D structures of the type of interest here, while other have "low dimensional" or somewhat open structures that are not strictly 2D. [64, 68] Given the impressive superconductivity in the TNCl class, doping these materials may well provide unusual insulator-metal transitions and perhaps some impressive superconductors.

6   Transition metal dichalcogenides and oxides: a class, or individuals?

Superconductivity has "emerged" is several layered transition metal oxides and dichalcogenides, including new members in the last decade or so. The unusual and perhaps unique, single band triangular lattice system, Li_xNbO_2 is discussed immediately below. This one, along with several others that have unusual characteristics, have $T_c \sim 5K$ as shown in Fig. 5. This range of T_c is not impressive in itself, but the observation that superconductivity continues to pop up in strongly 2D TM oxides and chalcogenides where correlation effects are moderate to strong, suggests new physics. The systems we will mention, although the discussion will be brief, are shown in Fig. 5, versus date of discovery. These materials do not seem to be very strongly connected to the cuprates (perhaps not at all), where T_c is a factor of 20-25 greater. But there are several examples. In the dichalcogenides, superconductivity arises in the same sort of systems, if not the same systems, where charge density waves (CDWs) and spin density waves (SDWs) are observed. These systems – at least the SDW members – display ordering wavevectors that are connected with Fermi surface calipers, and therefore are considered as Fermi surface instabilities. However, they are instabilities at q away from $\vec{q}$=0, whereas superconductivity is a $\vec{q} = \vec{k} - \vec{k}' = 0$ instability (because pairing couples $\vec{k}$ with $\vec{k}' = -\vec{k}$) since no translational symmetry is broken. Although superconductivity with pairing wavevector q different from zero is discussed more and more, this exotic FFLO (Fulde-Farrell-Larkin-Ovchinnikov [69,70]) type of pairing is yet to be established in any system. The main idea behind FFLO pairing, for a sys-
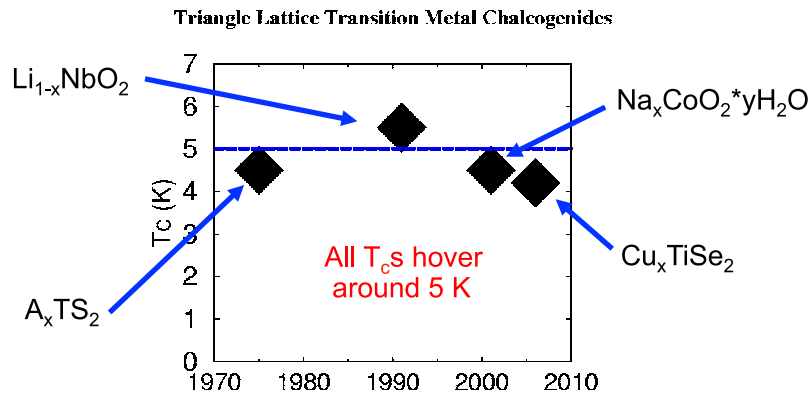
Synopsis: T_c in 2D Triangular Oxides/Chalcogenides

Triangle Lattice Transition Metal Chalcogenides

Fig. 5: *Display of four classes of layered transition metal dioxides or dichalcogenides, showing T_c versus year of discovery. Each has its specific peculiarities: the dichalcogenides also host spin- and charge-density waves; the niobate is a unique single band triangular lattice system; the cobaltate must be hydrated to become superconducting. Their critical temperatures are all in the neighborhood of 5K.*

tem with spin imbalance and thus somewhat different up and down FSs, is that a loss of kinetic energy by forming pairs with non-zero center of mass can be compensated by retaining partial "nesting" of electron and hole FSs.

6.1 Li_xNbO_2: a triangular lattice, single band correlated superconductor

The discovery of HTS in the cuprates in 1986 enlivened interest not only in layered cuprates but also in layered transition metal oxides more generally. The cuprates provided many-body theorists with a palette to study strong correlation effects in doped 2D antiferromagnets within a single band model. The intricate physics that occurs in the low carrier density regime has come at the cost of a more direct effort to focus on identifying the pairing mechanism. (In more recent times multiband models have become more popular for the cuprates.)

Another favorite of many-body modelers is the triangular lattice, because with antiferromagnetic coupling magnetic order (in addition to simple charge and orbital order) is frustrated, and the observed or calculated phenomena become very rich. However, true single band systems are sparse, and finding one on a triangular lattice is rare indeed.

In 1990 Geselbracht *et al.* [71,72] reported superconductivity up to 5.5 K in the Li_xNbO_2 system, synthesized and characterized structurally earlier by Meyer and Hoppe. [73] This system has been found [74] to be a single Nb $4d$ band, triangular lattice system, and one which promises to display correlated electron behavior [75] because the calculated bandwidth is smaller than the anticipated intraatomic repulsion U on Nb. At stoichiometry, $LiNbO_2$ should be a d^2 low-spin (i.e. nonmagnetic) ionic band insulator. With all Li removed (x=0 at fixed layered structure, see below), NbO_2 would be a d^1 compound and an excellent candidate as a Mott insulator; however, a rutile-related crystal structure is energetically favored in this limit. At intermediate concen-
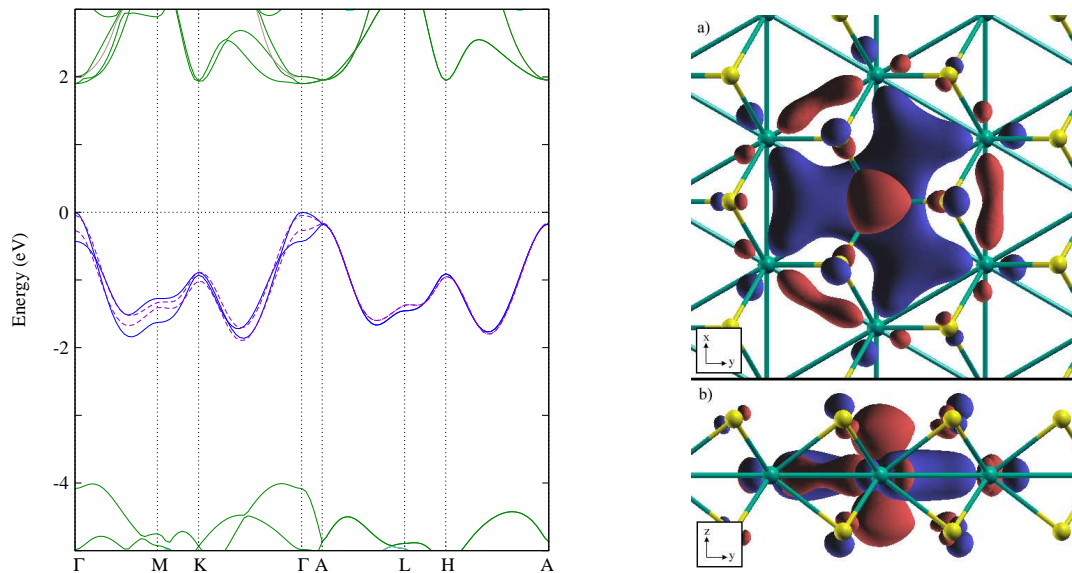
Fig. 6: *Left panel: Band structure of LiNbO$_2$ for the experimental structure. The two central Nb d_{z^2} bands arise from the two Nb atoms in the unit cell, and lie within a 6 eV gap separating the valence O $2p$ bands from the other Nb $4d$ bands above. The result is a triangular lattice single band system. Right panel: Isosurface plot of the the d_{z^2}-symmetry Wannier function. The top subpanel provides a top view, revealing the large "fan blades" extending toward neighboring Nb ions, represented by small aqua-colored spheres. The bottom subpanel shows the d_{z^2} lobe projecting perpendicular to the Nb layers, and small contributions from neighboring O ions. Red and blue indicate opposite signs of the Wannier function. The Wannier function as a whole has "s-like" (fully symmetric) symmetry of the Nb site.*

trations it should conduct, unless charge order or some other exotic phase arises at certain band fillings.

This is, so far, a single member class – a unique example; cuprates after all have several subclasses and dozens of members – which unfortunately has seen little further experimental study [76] but a fair amount of theoretical investigation. [74, 75, 77–79] The charge carriers hop amongst the Nb sites, which form a triangular lattice such that electron dispersion is strongly two dimensional. [74] The unique aspect is that the triangular prismatic coordination creates a strong crystal field that leaves the $4d_{z^2}$ orbital lowest in energy and well separated from the other $4d$ bands above and the O $2p$ bands below. It becomes a single band, triangular lattice system with formal charge Nb$^{(4-x)+}$: d^{1+x}. As mentioned above, the x=0 limit, which is not reached experimentally, corresponds to a triangular lattice Mott insulator according to the anticipated parameters [74] for this system: Hubbard U of 3-4 eV, DFT bandwidth of 1 eV. The observed T$_c$ up to 5.5 K is reported to be insensitive to the band filling, according to the (somewhat sparse) data.

Being a very light element, Li is almost invisible to xrays and, when samples are not of ideal quality (as these are not), Li concentration must be determined by other means. The multiphase nature of samples results in further uncertainty in the Li content of a given phase. Two other methods of doping the NbO$_2$ layer have been reported. One is that H is introduced into LiNbO$_2$.

The same T_c=5.5 K results, and the supposition by Kumada *et al.* [80] is that this procedure also produces hole-doping (from the stoichiometric x=1 compound), presumed to be due to formation of H^-. This supposition needs confirmation. In addition, $Mg_{0.5}NbO_2$ has been synthesized; this compound is structurally "identical" [81] to isovalent $LiNbO_2$. A sharp negative swing in the susceptibility occurred at 4.4 K, but the authors declined to interpret this necessarily as superconductivity (although a small volume fraction of superconductivity seems to be another possible source). It is intriguing to note that $Mg_{0.5}NbO_2 \equiv MgNb_2O_4$ has one more electron per transition metal than LiV_2O_4, which is one of the very few $3d$ based heavy fermion compounds. The theoretical studies strongly suggest that the conducting phases of Li_xNbO_2 should be rather strongly correlated.

In 2009 a startling development in this system was announced. Xue *et al.* [82] reported values of T_c in the 14-17 K range, three times larger than earlier reports while at compositions. Purity of the samples was sufficient to rule out $NbC_{1-y}N_y$, which has T_c in this same range, as the origin of the superconductivity. Moreover, the volume fraction of superconductivity was sufficient also to rule out the carbonitride phase. If confirmed (data always need independent confirmation) this higher range of T_c makes Li_xNbO_2 a much more interesting and important case.

6.2 Na_xCoO_2

This celebrated and heavily studied system is frustrating, in both senses of the word. As for the other triangular lattice compounds covered in this section, the transition metal (Co) sublattice [83] is frustrated for AFM coupling: the simplest way to see this is to note that around a triangle spin ordering cannot proceed up-down-up-down because the 1st and 4th sites are the same. This fact, and extensions that arise from it, form the core of much of the interest in triangular lattice systems. Na_xCoO_2 is doubly frustrating for those hoping to understand its behavior because the superconductivity itself continues to present awkward aspects. Two criteria are necessary for superconductivity to appear: (1) the Na concentration must be near (usually somewhat larger than) $x \sim 1/3$, and (2) the sample must be hydrated (*i.e.* dropped in water, or otherwise exposed to a great deal of water vapor H_2O). The observation that x=1/3 might be special is that there is a strong tendency in such a system, if strongly correlated, toward $\sqrt{3} \times \sqrt{3}$ charge and/or spin ordering (and perhaps orbital ordering), as predicted [84] by correlated band theory studies. Ordering is also predicted at half filling, and indeed an ordered, Mott insulating phase is observed at x=1/2. The frustrating thing is that it remain mysterious what incorporation of H_2O does – beyond the expectation that the molecule decomposes – but it is essential for superconductivity.

It is not in the purview of this paper to survey the extensive experimental work on this system, nor the also rather extensive theoretical work. We do however point out that several experimental studies have tried to ascertain the *oxidation state* of the Co ion, versus the "doping level" of Na (x). All have concluded that the oxidation state of Co is characteristic of a doping level (Na concentration plus things that H_2O might cause) of $x_{eff} \sim 0.55$-60, that is, moderately electron-doped above half filling of the relevant Co $3d$ band. This system remains a conundrum, one for

which there are few if any solid models.

6.3   Doped transition metal dichalcogenides; recently $Cu_x TiSe_2$

This transition metal dichalcogenide class of quasi-2D materials, mostly metals, has a long history and large literature. Many examples of CDW and SDW materials occur in this system, and a glimpse of the many phenomena that occur in this system can be obtained from a recent report on $1T\text{-}Ta_{1-x}Fe_xS_2$, [85] which contains a normal metal phase at high temperature and charge-ordered, superconducting, and correlated insulator phases at lower temperature. (The "1T," "2H," etc. designations indicate symmetry and stacking of the TaS_2 motifs.) SDW materials usually have a magnetic order wavevector that can be identified with a Fermi surface caliper. The same had been suggested for CDW phases early on, and presumed for many years, since the generalized (Lindhard) susceptibility is expected to peak at wavevectors spanning the Fermi surface. This viewpoint has been questioned in recent years, and the complexity of the phase diagrams in dichalcogenides rivals those of oxides. Calculations of the susceptibility, including the relevant matrix elements, seem in several cases not to bear out earlier expectations: CDW wavevectors and Fermi surface calipers sometimes do not match up. [86] Recent evidence indicates that states not only near the Fermi surface but also some distance away (on an eV energy scale) contribute almost as heavily.

The electron-doped system $Cu_x TiSe_2$ system has caused some attention to return to this class of materials. The doping by Cu is proposed to allow study of the relevant phase diagram via simple (synthetic) means; [87] however, the solubility limit is only 11% for this compound. The superconducting T_c peaks in this system just above 4 K. The many questions greatly outweigh the few answers. One important experimental result is that the superconductivity is reported to be s-waver; [88] given the plethora of indications that electronic correlation effects are strong in this system, this "conventional" form of gap should not be interpreted as a strong indicator of electron-phonon pairing.

7   NaAlSi: an unusual self-doped semimetallic superconductor

Occasionally a semimetal is encountered that is self-doped: a semimetal arising from "accidentally" overlapping bonding valence and antibonding conduction bands. It was noted in Sec. 4 that MgB_2 can also be regarded as a self-doped semimetal. Much more occasionally such a material is a superconductor; elemental Bi with its distorted fcc lattice it a well known, though not understood, example. NaAlSi which superconducts [89] at 7 K, interestingly possesses the crystal structure of the "111" iron pnictide superconductors although their electronic structures have nothing in common. Another intriguing, but surely irrelevant, aspect of this compound is that moving each element to the next higher row (smaller Z, but isoelectronic) gives LiBC, the MgB_2-like materials that was discussed briefly earlier in this article.
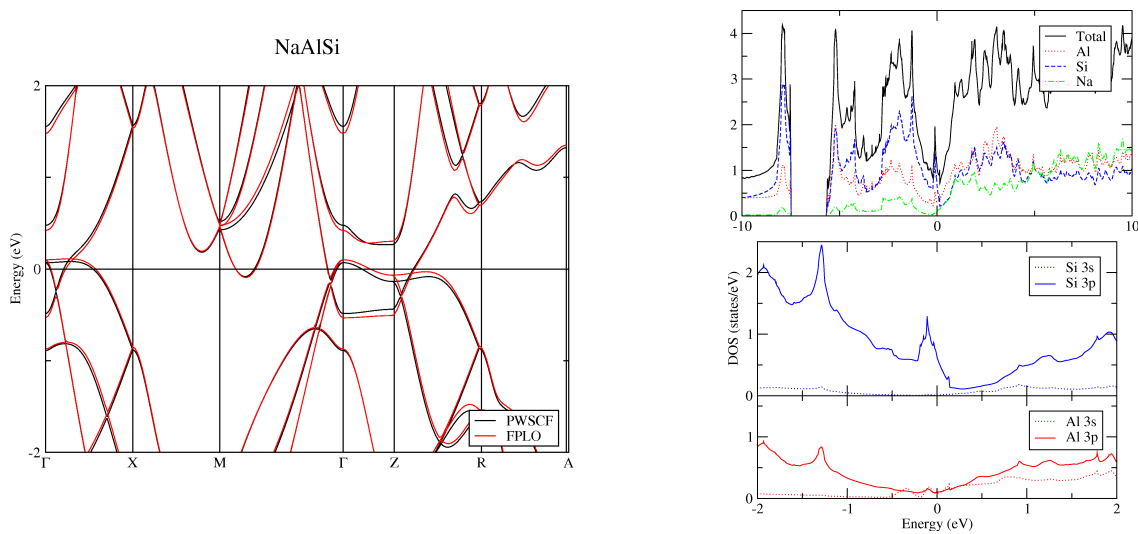
Fig. 7: *Left panel: Density functional based band structure of NaAlSi near the Fermi level. The band structure was calculated with the two methods (all-electron, and pseudopotential) that are designated in the caption. The conduction bands at and above the Fermi level are strongly Al in character, while the band extending below the Fermi level are Si-derived. The energy scale is in eV. Right panel: Pictured in a 20 eV wide region, the total and atom- and orbital-projected density of states of NaAlSi. Note the pseudogap around the Fermi energy, with the sharp peak at the minimum. The middle subpanel provides an expanded view of the very narrow and sharp peak spanning the Fermi energy. The lower subpanel shows no contribution of Al states to the density of states peak.*

Structurally, the $AlSi_4$ tetrahedra replace the $FeAs_4$ tetrahedra that forms the basic feature of the "111" materials, while the buckled layer of interstitial Na ions simply contributes their electrons to the Al-Si bands. This provides 8 valence electrons/f.u., which encourages covalent bonding and the formation of bonding valence and antibonding conduction bands. This indeed occurs although a simple characterization of the bonding-antibonding distinction has not yet been constructed. It is established that the bonding bands are strongly Si in character while the conducting bands are primarily Al. The gap is small, however, and the bands overlap slightly [90] near $\vec{k}=0$ giving a semimetallic band structure.

The resulting density of states, shown in Fig. 7, is predicted from DFT studies to display an extremely sharp and narrow peak overlapping the Fermi level. [90] The scale of strong variation of N(E) is similar to that of the largest phonon frequency, implying that the Born-Oppenheimer approximation underlying el-ph theory and hence Eliashberg theory cannot necessarily be relied on. The superconductivity in NaAlSi requires further developments in theory. An attempt to evaluate the el-ph coupling strength using conventional theory (including the Born-Oppenheimer approximation) was thwarted by the small Fermi surfaces, which requires finer $\vec{k}$ and $\vec{Q}$ mesh than was possible with even rather large computer clusters and memories.

Another conundrum is presented by this system. The isostructural and isovalent sister compound NaAlGe has also been synthesized. It's electronic structure is virtually identical to that of NaAlSi. Nonetheless, it is found not to be superconducting (above 2 K). This fact revives
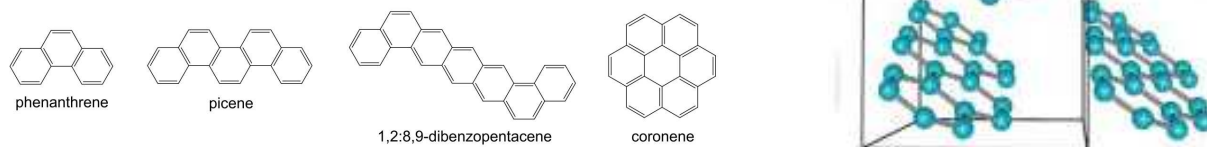
Fig. 8: *Left panel: Structures of the four hydrocarbon molecules that, when condensed to crystalline form and electron-doped with alkali atoms, superconduct. The coronene closed wheel of benzene rings is structurally distinct from the other "benzene chains." Right panel: Crystal structure of picene, showing the herringbone alignment of molecules; only carbon atoms are pictured in both panels. The box outlines a primitive cell. The non-intuitive orientation and alignment of molecules results in the low symmetry monoclinic $P2_1$ space group.*

the question occurring in the HfNCl and ZrNCl system: can the difference in superconducting behavior arise from the small and seemingly negligible differences in the electronic structure, or is it due to the mass difference – in this case Ge (73 amu) versus Si (28 amu), or to some other as yet undetermined origin. Another point of interest that we mention in passing is the relation, or perhaps not, to its relative CaAlSi [91, 92] that has one more valence electron.

8   Doped hydrocarbons: organic crystals

A recent development, since the data used for Fig. 1 was available and which is only now beginning to create a stir, is the demonstration of T_c up to 33K in electron-doped hydrocarbon solids. Superconductivity in organometallic compounds has been under study for well over two decades, and the originally low values of T_c had been raised to the 10K regime. For reviews see the book by Ishiguro, Yamaji, and Saito [93] and the overview by Jerome. [94] These materials are strongly 2D in their electronic properties, and seem to show a combination of considerable correlated electron behavior as well as strong electron-phonon coupling. A coherent picture is lacking.

The recent developments center on molecular solids build on aromatic hydrocarbon molecules phenanthrene $C_{14}H_{10}$, picene $C_{22}H_{14}$, and dibenzopentacene $C_{30}H_{18}$, comprising three, five, and seven connected benzene rings, respectively. For $K_x$picene, T_c up to 18 K was reported in 2010 by Mitsuhashi *et al.* [95], and this has been followed by Xue *et al.* in 2012 reporting T_c=33 K in $K_x$dibenzopentacene. [96] These latter authors have noted that the maximum T_c so far appears to be linear in the number of benzene rings (each ring adding $\sim$7 K) and they suggest that "delocalization" of the conduction electron wavefunctions over the molecule is a relevant factor. These molecules are sometimes described heuristically as tiny flakes or ribbons of of H-capped graphene; however, they differ in containing C-C double bonds, see Fig. 8.

These systems, especially the picene-based one, is attracting active study from both experimen-

talists and theorists, and an overview is inadvisable at this time. It is relevant to this article however that density functional based linear response calculation of the phonon dispersion and electron-phonon interaction strength and spectral distribution have been reported by Subedi and Boeri. [97] They obtain strong coupling to H-C bend modes and 1400 cm^{-1} and C-C stretch modes around 1600 cm^{-1}, and for various doping levels obtain coupling strength values in the range $\lambda \approx 0.65 - 0.75$, which is enough to account for the observed values of T$_c$. Whether these materials are really Fermi liquid metals (needed for the validity of Eliashberg theory) is currently being explored using several experimental techniques.

9   Summary of main points

From the data shown in Fig. 1, two dimensionality clearly seems to be special in producing classes of high temperature superconductors. Doped insulators account for a substantial number of these classes; the insulators my be either magnetic insulators (cuprates) or band insulators ($\mathcal{T}$NCl). Beyond these two categories, the phenomena (and likely the pairing mechanisms) vary. The doped nitridochlorides do not display indications of the usual sort of strong electron correlation (enhancements; magnetic moments), which the doped insulators discussed in Sec. 6 fall within the categorization of electronically correlated materials. It is well recognized that the strongly correlated systems require more extensive study and that pairing mechanisms remain to be identified. One of the main purposes of this article is to point out that the transition metal nitridochlorides and similar materials are different, and seem to require their own distinct means of pairing.

10   Acknowledgments

References

[1] J. Bardeen, L. N. Cooper, and J. R. Schrieffer, Phys. Rev. **108**, 1175 (1957).

[2] L. N. Cooper, Phys. Rev. **104**, 1189 (1956).

[3] J. R. Schrieffer, *Superconductivity* (Benjamin, New York, 1964).

[4] P. B. Allen, Phys. Rev. B **13**, 1416 (1976).

[5] W. Kohn and J. M. Luttinger, Phys. Rev. Lett. **15**, 524 (1965).

[6] R. Joynt and L. Taillefer, Rev. Mod. Phys. **74**, 235 (2002).

[7] G. M. Eliashberg, Zh. Eksperim. Teor. Fiz. **38**, 966 (1960) [English transl.: Soviet Phys. JETP **11**, 696 (1960)].

[8] D. J. Scalapino, J. R. Schrieffer, and J. W. Wilkins, Phys. Rev. **148**, 263 (1966).

[9] P. Hohenberg and W. Kohn, Phys. Rev. **136**, B864 (1964).

[10] W. Kohn and L. J. Sham, Phys. Rev. **140**, A1133 (1965).

[11] P. B. Allen and R. C. Dynes, Phys. Rev. B **12**, 905 (1975).

[12] P. M. Platzman and T. Lenosky, Phys. Rev. B **52**, 10327 (1995).

[13] Y. Takano, T. Takenouchi, S. Ishii, S. Ueda, T. Okutsu, I. Sakaguchi, H. Umezawa, H. Kawarada, and M. Tachiki, Diamond & Related Mat. **16**, 911 (2006).

[14] W.E. Pickett, Physica C **468**, 126 (2008).

[15] J. K. Jain and P. B. Allen, Phys. Rev. Lett. **54**, 2437 (1985).

[16] P. B. Allen, M. L. Cohen, and D. R. Penn, Phys. Rev. B **38**, 2513 (1988).

[17] A. Bill, H. Morawitz, and V. Kresin, Phys. Rev. B **66**, 100501 (2002).

[18] A. Bill, H. Morawitz, and V. Kresin, Phys. Rev. B **68**, 144519 (2003).

[19] I.N. Askerzade and B. Tanatar, Physica C **420**, 11 (2005).

[20] C. Falter and G. A. Hoffmann, Phys. Rev. B **64**, 054516 (2001).

[21] C. Falter, Phys. Stat. Sol. (b) **242**, 78 (2005).

[22] G. S. Atwal and N. W. Ashcroft, Phys. Rev. B **70**, 104513 (2004).

[23] J. Nagamatsu, N. Nakagawa, T. Muranaka, Y. Zenitani, and J. Akimitsu, Nature **410**, 63 (2001).

[24] J.M. An and W.E. Pickett, Phys. Rev. Lett. **86**, 4366 (2001).

[25] J. Kortus, I.I. Mazin, K.D. Belashchenko, V.P. Antropov, and L. L. Boyer, Phys. Rev. Lett. **86**, 4656 (2001).

[26] K.D. Belashchenko, M. van Schilfgaarde, and V.P. Antropov, Phys. Rev. B **64**, 092503 (2001).

[27] Y. Kong, O. V. Dolgov, O. Jepsen, and O. K. Andersen, Phys. Rev. B **64**, 020501 (2001).

[28] A. Liu, I. I. Mazin, and J. Kortus, Phys. Rev. Lett. **87**, 087005 (2001).

[29] W. E. Pickett, J. Supercond. & Novel Magn. **19**, 291 (2006).

[30] M. Wörle, R. Nesper, G. Mair, M. Schwarz, and H. G. von Schnering, Z. Anorg. Allg. Chem. **621**, 1153 (1995).

[31] H. Rosner, A. Kitaigorodsky, and W. E. Pickett, Phys. Rev. Lett. **88**, 127001 (2002).

[32] J. M. An, S. Y. Savrasov, H. Rosner, and W. E. Pickett, Phys. Rev. B **66**, 220502 (2002).

[33] A. M. Fogg, G. R. Darling, J. B. Claridge, J. Meldrum, and M. J. Rosseinsky, Phil Trans. Roy. Soc. A **366**, 55 (2008).

[34] A. Lazicki, C. S. Yoo, H. Cynn, W. J. Evans, W. E. Pickett, J. Olamit, K. Liu, and Y. Ohishi, Phys. Rev. B **75**, 054507 (2007).

[35] J. An and W. E. Pickett, unpublished.

[36] M. Wörle and R. Nesper, J. Alloys Compounds **216**, 75 (1994).

[37] P. Ravindran, P. Vajeeston, R. Vidya, A. Kjekshus, and H. Fjellvag, Phys. Rev. B **64**, 224509 (2001).

[38] H. Harima, Physica C **378-381**, 18 (2002).

[39] A. K. Verma, P. Modak, D. M. Gaitonde, R. S. Rao, B. K. Godwal, and L. C. Gupta, EPL **63**, 743 (2003).

[40] E. Spano, M. Bernasconi, and E. Kopnin, Phys. Rev. B **72**, 014530 (2005).

[41] S. Lebegue, B. Arnaud, and M. Alouani, Comp. Mat. Sci. **37**, 220 (2006).

[42] T. Mori and E. Takayama-Muromachi, Current Appl. Phys. **4**, 276 (2004).

[43] H. Y. Yan, M. G. Zhang, Q. Wei, and P. Guo, Comp. Mat. Sci. **68**, 174 (2013).

[44] K. Hoffman, X. Rocquefelte, J. F. Halet, C. Bahtz, and B. Albert, Angew. Chemie - Intl. Ed. **47**, 2301 (2008).

[45] A. H. Moudden, Eur. Phys. J. B **64**, 173 (2008).

[46] E. R. Ylvisaker and W. E. Pickett, unpublished.

[47] B. Albert and K. Schmitt, Inorg. Chem. **38**, 6159 (1999).

[48] M. Somer, A. Yarasik, L. Akselrud, S. Leoni, H. Rosner, W. Schnelle, and R. Kniep, Angew. Chem. - Int. Ed. **43**, 1088 (2004).

[49] S. Yamanaka, H. Kawaji, K. Hotehama and M. Ohashi, Adv. Mater. **9**, 771 (1996).

[50] S. Shamoto, T. Kato, Y. Ono, Y. Miyazaki, K. Ohoyama, M. Ohashi, Y. Yamaguchi, and T. Kajitani, Physica C **306**, 7 (1998).

[51] S. Yamanaka, K. Hotehama and H. Kawaji, Nature **392**, 580 (1998).

[52] S. Shamoto, T. Kato, Y. Ono, Y. Miyazaki, K. Ohoyama, M. Ohashi, Y. Yamaguchi, and T. Kajitani, J. Phys. Chem. Solids (1998, in press).

[53] M. Ohashi, S. Yamanaka, and M. Hattori, J. Ceram. Soc. Jpn. Int. Ed. **97**, 1175 (1989).

[54] S. Yamanaka, T. Yasunaga, K. Yamaguchi, and M. Tagawa, J. Mater. Chem. **19**, 2573 (2009).

[55] A. Kaur, E. R. Ylsivaker, Y. Li, G. Galli, and W. E. Pickett, Phys. Rev. B **82**, 155125 (2010).

[56] Y. Taguchi, A. Kitora, and Y. Isawa, Phys. Rev. Lett. **97**, 107001 (2006).

[57] C. M. Schurz, L. Shlyk, T. Schleid, and R. Niewa, Zeitschrift f. Krist. **226**, 395 (2011).

[58] R. Weht, A. Filippetti, and W. E. Pickett, EPL **48**, 320 (1999).

[59] R. Heid and K. P. Bohnen, Phys. Rev. B **72**, 134527 (2005).

[60] R. Akashi, K. Nakamura, R. Arita, and M. Imada, Phys. Rev. B **86**, 054513 (2012).

[61] E. R. Ylvisaker and W. E. Pickett, EPL **101**, 57006 (2013).

[62] Y. Taguchi, Y. Kasahara, T. Kishume, T. Takano, K. Kobayashi, E. Matsuoka, H. Onodera, K. Kuroki, and Y. Iwasa, Physica C **470**, S598 (2010).

[63] Q. Yin, E. R. Ylvisaker, and W. E. Pickett, Phys. Rev. B **83**, 014509 (2011).

[64] D. A. Headspith and M. G. Francesconi, Topics Catal. **52**, 1611 (2009).

[65] T. Takasaki, T. Ekino, H. Fujii, and S. Yamanaka, J. Phys. Soc. Japan **74**, 2586 (2005).

[66] Y. Taguchi, T. Kawabata, T. Takano, A. Kitora, K. Kato, M. Takata, and Y. Isawa, Phys. Rev. B **76**, 064508 (2007).

[67] D. H. Gregory, M. G. Barker, P. P. Edwards, and D. J. Siddons, Inorg. Chem. **35**, 7608 (1996).

[68] D. H. Gregory, P. M. O'Meara, A. G. Gordon, D. J. Siddons, A. J. Blake, M. G. Barker, T. A. Hamor, and P. P. Edwards, J. Alloys Compds. **317-318**, 237 (2001).

[69] P. Fulde and R. A. Ferrell, Phys. Rev. **135**, A550 (1964).

[70] A. I. Larkin and Yu. N. Ovchinnikov, Zh. Eksp. Teor. Fiz. **47**, 1136 (1964).

[71] M. J. Geselbracht, T. J. Richardson, and A. M. Stacy, Nature **345**, 324 (1990).

[72] M. J. Geselbracht, A. M. Stacy, A. R. Garcia, B. G. Silbernagel, and G. H. Kwei, J. Phys. Chem. **97**, 7102 (1993).

[73] G. Meyer and R. Hoppe, J. Less-Common Metals **46**, 55 (1976).

[74] E. R. Ylvisaker and W. E. Pickett, Phys. Rev. B **74**, 075104 (2006).

[75] K.-W. Lee, J. Kuneš, R. T. Scalettar, and W. E. Pickett, Phys. Rev. B **76**, 144513 (2007).

[76] E. G. Moshopoulou, P. Bordet, and J. J. Capponi, Phys. Rev. B **59**, 9590 (1999).

[77] G. T. Liu, J. L. Luo, Z. Li, Y. Q. Guo, N. L. Wang, D. Jin, and T. Xiang, Phys. Rev. B **74**, 012504 (2006).

[78] E. R. Ylvisaker, K.-W. Lee, and W. E. Pickett, Physica B **383**, 63 (2006).

[79] D. L. Novikov, V. A. Gubanov, V. G. Zubkov, and A. J. Freeman, Phys. Rev. B **49**, 15830 (1994).

[80] N. Kumada, S. Watauchi, I. Tanaka, and N. Kinomura, Mater. Res. Bull. **35**, 1743 (2000).

[81] A. Miura, T. Takei, and N. Kumada, J. Solid State Chem. **197**, 471 (2013).

[82] Z. Xue, A. Dong, Y. Guo, and G. Che, J. Alloys Compds. **476**, 519 (2009).

[83] G. Meyer and R. Hoppe, Angew. Chem., Int. Ed. Engl. **13** (1974); J. Less-Common Met. **46**, 55 (1976).

[84] K.-W. Lee and W. E. Pickett, Phys. Rev. Lett. **96**, 096403 (2006).

[85] R. Ang, Y. Tanaka, E. Ieki, K. Nakayama, T. Sato, L. J. Li, W. J. Lu, Y. P. Sun, and T. Takahashi, Phys. Rev. Lett. **109**, 176403 (2012).

[86] M. D. Johannes and I. I. Mazin, Phys. Rev. B **77**, 165135 (2008).

[87] E. Morosan, H. W. Zandbergen, B. S. Dennis, J. W. G. Bos, Y. Onose, T. Klimczuk, A. P. Ramirez, N. P. Ong, and R. J. Cava, Nat. Phys. **2**, 544 (2006).

[88] S. Y. Li, G. Wu, X. H. Chen, and L. Taillefer, Phys. Rev. Lett. **99**, 107001 (2007).

[89] S. Kuroiwa, H. Kawashima, H. Kinoshita, H. Okabe, and J. Akimitsu, Physica C **466**, 11 (2007).

[90] H. B. Rhee, S. Banerjee, E. R. Ylvisaker, and W. E. Pickett, Phys. Rev. B **81**, 245114 (2010).

[91] H. Sagayama, Y. Wakabayashi, H. Sawa, T. Kamiyama, A. Hoshikawa, S. Harjo, K. Uozato, A. K. Ghosh, M. Tokunaga, and Tamegai, J. Phys. Soc. Jpn. **75**, 043713 (2006).

[92] S. Kuroiwa, H. Sagayama, T. Kakiuchi, H. Sawa, Y. Noda, and J. Akimitsu, Phys. Rev. B **74**, 014517 (2006).

[93] T. Ishiguro, K. Yamaji, and G. Saito, *Organic Superconductors*, Springer Series in Solid State Sciences (Springer-Verlag, Berlin, 1998).

[94] D. Jérome, Chem. Rev. **104**, 5565 (2004).

[95] R. Mitsuhashi, Y. Suzuki, Y. Yamanari, H. Mitamura, T. Kambe, N. Ikeda, H. Okamoto, A. Fujiwara, M. Yamaji, N. Kawasaki, Y. Maniwa, and Y. Kubozono, Nature **464**, 76 (2010).

[96] M. Xue, T. Cao, D. Wang, Y. Wu, H. Yang, X. Dong, J. He, F. Li, and G. F. Chen, Sci. Rep. **2**, 389 (2010).

[97] A. Subedi and L. Boeri, Phys. Rev. B **84**, 020508 (2011).